DISTRIBUTED COMPOSITIONAL AND TEMPERATURE NATURE OF MELTS IN SUBMERGED AND OPEN ARC FURNACES IN HIGH CARBON FERROCHROME PRODUCTION

J.J. Eksteen[1], S.J. Frank[1] and M.A. Reuter[2]

[1]University of Stellenbosch, Department of Process Engineering, Private Bag X1, Matieland, 7602, South Africa.
E-mail: jeksteen@ing.sun.ac.za
[2]Delft University of Technology, Department of Applied Earth Sciences Mijnbouwstraat 120,
2628 RX Delft, The Netherlands. E-mail: M.A.Reuter@citg.tudelft.nl

ABSTRACT

The development of feedforward semi-empirical control models for furnaces and the evaluation of mass balances are based on plant data. The models can only be as good as the data and it is therefore required to know the inherent uncertainty associated with the plant data. This uncertainty stems mainly from the fact that the slag, alloy or dust, have a distributed nature that depends on the degree of mixedness. It is commonly accepted that melts from open bath furnaces are well-mixed, and submerged arc furnaces less so. The impact of this assumption is significant, as a reasonably homogeneous melt could be represented by one sample only. As so much of metallurgical control depends on the assay information of the alloy and slag melts from furnaces, it was decided to characterise the possible variation in melt chemistry and temperature. Sampling campaigns and continuous temperature measurement of the melts were performed for different alloy and slag taps at a major ferrochrome producer. Both a submerged arc furnace and open arc furnace are evaluated in this way, by way of comparison. The slags of both open arc and submerged arc furnaces were found to be of similar degrees of homogeneity, with much spatial variance in the reducible iron and chromium oxides. However, it was found that the alloy melts deriving from open arc furnaces were significantly less homogeneous than the alloy derived from submerged arc furnace alloy production. The compositional variance could be related to the furnace operating conditions and it affects both metallurgical accounting and process control. In all cases it was found that the variance in melt solute components are larger than can be ascribed to analysis instrument error. It will be shown how this predetermined variance in melt composition could be included in process modelling and control.

1. INTRODUCTION

To improve and optimise the production in industrial ferro-alloy furnaces, one firstly requires a steady state mass balance as a baseline and secondly a dynamic model to predict the product quality, composition and yield that can be expected for a future tap. However, material balance closure is seldom possible based on raw data. Furthermore, without material balance closure, further modelling makes little sense. Material balance closure can be obtained within the inherent uncertainty of the data, based on data reconciliation techniques, as has been shown by the authors [1]. Unless gross sampling errors occurred, the inherent uncertainty in material assays is directly related to the mixedness of the material sampled. Mixedness therefore has to be quantified before any further modelling can take place. Without knowledge of the state of mixedness (and therefore uncertainty), the best thermodynamic, fundamental or systems models become irrelevant. It has also been shown by the authors that, once the spatial distributions are known and the data has been reconciled within its natural variance, thermodynamic and systems modelling can be done successfully [2], [3]. These models can then predict the composition and yield associated with a future tap within the precision of the measurements [3][4]. As the modelling tools have been developed by the authors to use reconciled data, one needs to quantify only the mixedness of the system of interest.

A number of computational fluid dynamic (CFD) modelling and physical modelling evaluations have been performed on arc furnaces that lead one to believe that the melts are well mixed [5], [6], [7], [8], [9]. The combination of gas generation and bubbling though the melt, natural convection, plasma arc impingement and electro-hydrodynamic driving forces constitute an ensemble of forces acting on the melt to induce fluid flow. However, very little has been published regarding actual industrial measurements to characterise the mixing in open arc and submerged arc furnaces. Neither have any mixedness comparisons been published with regard to the same smelter plant performing both open arc bath reductive smelting and submerged arc reductive smelting of chromite ores. This paper addresses thermal and compositional mixedness of industrial furnaces, using statistical analysis to characterise the distributiveness of species concentrations and temperature. It would be useful to determine which operating conditions or physico-chemical conditions contribute significantly to the degree of homogeneity, to establish what could be done to influence the degree of mixing.

Once the degree of mixedness has been characterised, it will be useful to incorporate this information in the way we handle the industrial data to develop process models, taking into account that the uncertainty of an assay with respect to the bulk composition of a melt is directly related to the homogeneity of the melt if the analysis instrument error is low.

2. ASSESSING MIXTURE QUALITY

Good melt mixedness can be identified with a melt showing very little thermal and compositional variance through the melt volume. A tracer in a liquid is well mixed with the liquid once the tracer has a relative composition variation of less than 5% relative to the bulk average tracer concentration [10].

To determine mixedness, a tracer is typically introduced as a pulse into a homogeneous liquid in which it is soluble in all proportions. The "mixing time" is the time measured from the instant of addition, until the vessel contents have reached a specific degree of uniformity. The equilibrium concentration, C_∞ of a tracer of known volume can be calculated from a simple mass balance if is to be introduced into a melt / liquid of known volume. The mixing time may be defined as the time from the instant of tracer addition for the concentration of the tracer to reach a equilibrium value. However, the mixing time depends on the way of tracer addition and the location of the concentration detector. Moreover, the asymptotic approach of the equilibrium concentration makes it difficult to detect with precision.

In order to eliminate the influence of detector position, the concentration variance (or standard deviation) could be determined by taking a number of samples from different positions in the melt, at say n different locations. The population variance could be calculated as [10]:

$$\sigma^2 = \frac{1}{n-1}\sum_{i=1}^{n}(C_i - C_\infty)^2 \tag{1}$$

In the case where tracers or the ratio of tracer to liquid volume is unknown, one first needs to calculate the arithmetic average concentration (sample average), as an estimate of the equilibrium concentration (population average).

$$\overline{C} = \sum_{i=1}^{n}\frac{C_i}{n} \tag{2}$$

In such a case, the sample variance estimate is:

$$s^2 = \frac{1}{n-1}\sum_{i=1}^{n}\left(C_i - \overline{C}\right)^2 \tag{3}$$

If mixing time is now to be estimated, it can be done based on the point where the sample variances approaches zero. Although the effect of the location of the detector / sensor has been eliminated, the asymptotic nature of the approach is still present. Consequently, the time to achieve 5% relative variation is taken as the mixing time [10]. In the case of sampling from a melt during tapping, Eq. (2) and (3) will be used to calculate the average and sample variance respectively.

Levenspiel [11] shows how to estimate the break-up time of macro fluids according to Einstein's random walk equation:

$$t = \frac{(Size\ of\ element)^2}{(Diff.\ Coeff.)} = \frac{d_{element}^2}{D_{mass}} \tag{4}$$

It is shown [11], via Eq. (4), that for a dilute aqueous solution, a water element of 1 micron in size and a diffusion coefficient of 10^{-5} cm^2/s would lose its identity in one millisecond, but that a viscous polymer of 100 micron in size 1000 times as viscous as water would retain its identity for up to 3 hours. If it is taken into account that discrete mineral particles have to melt, intermix with other fluxes, be reduced, and that silicate polymers also exist within slag melts, it becomes apparent that fluid elements of slags may take a significant time to break down. The interaction between mixing with reactions becomes important when the time to become homogeneous is not short with respect to the time for reaction to take place. This is typically the case with very fast reactions and viscous reactant fluids[11]. In the case of molten bath systems, both very fast reactions occur, and the fluids could be viscous, especially when any of the melt temperatures are below the melt liquidus temperatures. This makes the fundamental predictability of reaction yields so much more difficult.

Mixing time as such is not of so much importance for furnaces already in operation (it is much more important during the furnace design stage). However, there is much sense in determining the variance in the composition at a given stage (say at tapping of the melt) and investigating the statistical properties of the variances over several taps. It would also be sensible to relate variance to the operating and metallurgical conditions of the furnace. However, taking many samples per tap for many taps is not only laborious, it is an expensive and inherently unsafe task, considering the practical aspect of drawing spoon samples from fast flowing melts above 1500°C. Furthermore, there is little sense in basing mixedness variance on species in the melt with a concentration of higher than say 5%, as one would then be analysing the solvent which inherently has a small sample variance, and not the trace or minor species. However, the determination of sampling variances of all species does have some importance as it gives an estimate of the relative certainty one can associate with a sample.

Harnby et al. [10] mentions that the most relevant description of mixing processes in the process industry is the variation coefficient, or relative coefficient of variation, s_{rel}:

$$s_{rel} = \sqrt{\frac{s^2}{\overline{C}^2}} \tag{5}$$

As the relative standard deviation, s_{rel}, of assaying and chemical analysis is seldom more than 2%, one may compare the relative standard deviation associated with sampling to the inherent analytical instrument variance. Thereby one can determine if sampling variance is associated with the analyses instrument only, or if the variance was already present in the melt due to poor mixing. Eq. (5) will be used through the remainder of the paper as the standard basis to compare mixedness.

3. THERMAL VERSUS COMPOSITIONAL MIXEDNESS

While temperature variation with position can be used to quantify mixedness [10], for the purpose of estimating mixing times, it is of less value to determine mixedness on a meso and micro scale (as would applicable to solute components in a melt) and thermal mixedness cannot be extrapolated to compositional mixedness. One of the main reasons is the difference one finds between thermal diffusivity:

$$D_{thermal} = \frac{k_{thermal}}{\rho \cdot C_P} \tag{6}$$

and mass the diffusivities D_{ij}, which could be estimated from viscosity data or obtained from literature or experiment. Both could be stated in the SI units of m^2s^{-1}. Thermal energy is transferred up to an order of magnitude faster than molecules could move from one location to another, showing that a system could tend to thermal homogeneity, but still be far from compositional homogeneity. For a typical slag system found in reductive chromite smelting, consisting of MgO, CaO, Al_2O_3, SiO_2 and smaller amounts of FeO and CrO, one may investigate the relationship between thermal and mass diffusivity through lumping MgO, FeO and

CrO with CaO as "CaO", and investigating the ternary system CaO, SiO_2, Al_2O_3. This system approaches the system 40CaO: $20Al_2O_3$: $40SiO_2$ investigated by Turkdogan [13]. Various radioactive tracers have been used, such as the isotopes of ^{45}Ca, ^{31}Si and ^{26}Al. As Si is the only component appreciably reduced from CaO-Al_2O_3-SiO_2 slag to alloy, it would be worthwhile to look at Si behaviour in particular. Using the values given by Turkodogan [13], and as diffusivity follows an Arrhenius relationship, the pre-exponential factor was estimated at 70.0 cm^2s^{-1} and the diffusion activation energy as –288.5 kJ/mol, the diffusivity was estimated at 1550 °C as about 4.00×10^{-7} cm^2s^{-1}. Based on the information by Turkdogan [13], the effective thermal conductivity of these type of slags was noted to be 0.01 to 0.02 $W.cm^{-1}K^{-1}$, while the density was noted to be 2.58 $g.cm^{-3}$ and the specific heat was of the order 0.8-1.0 $J.g^{-1}K^{-1}$. Using the values above (average values in the case of ranges), the thermal diffusivity can be estimated to be about 7.3×10^{-3} cm^2s^{-1} in comparison with the mass diffusivity of 4.0×10^{-7} cm^2s^{-1}. The thermal diffusivity is therefore 1.8×10^5 times (5 orders of magnitude) as much as the mass diffusivity. This quick calculation demonstrates the significant difference between the rate of heat transfer in a melt and the rate of mass transfer.

4. MELT SPECIES MIXEDNESS

During normal operating practice, the slag and alloy are sampled once each, at any ad-hoc time, once the flow of the melt through the tapping launder is fully developed. To determine if significant spatial distributiveness exists with regard to the composition and temperature, two designated sampling campaigns were scheduled, where the temperature and compositions of the slag, alloy, and flue dust were monitored. For a number of slag and alloy taps, 6 equispaced samples were taken per tap, once the melt flow through the launder to the ladle was fully developed. These samples were all handled identically, with regard to quenching and assaying of the samples. All the sample sizes were similar and of the order of about 50-60 cm^3. A number of alloy and slag taps were also monitored using a Mikron M90 H pyrometer, mounted on a tripod and focused on the molten alloy at the tap hole during the tapping. The pyrometer, with a range from 600 °C to 3000 °C and a precision of 0.4% was calibrated using disposable dip thermocouples.

The slag samples were analysed using X-ray fluorescence spectrometry (XRF), while the alloy samples were analysed using a spark optical emission spectrometry (spark OES). Carbon and sulphur in all feed and product phases were analysed using a LECO CS200 analyser. It was found that the slag also contained carbon, even though no visible free carbon was present. It was assumed that the carbon in the slag derives from entrained alloy droplets which contain in the order of 8% carbon.

4.1 Alloy Homogeneity

Over and above the need to obtain an idea of tap composition variance for the purpose of furnace control and mixedness analysis, accurate assays of the contaminants in the ferrochrome alloy are especially important where ferrochrome and stainless steel plants are operated in close proximity, as there is currently a drive for "just-in-time" molten alloy transfer from the ferrochrome plants to the stainless steel plants. Analysis of the alloy samples (6 per tap) of high carbon ferrochrome (HCFeCr) proved that the HCFeCr alloy derived from a direct current plasma arc furnace (PAF) is, in general, not well mixed at all with respect to the solutes (assuming a solvent matrix of molten Cr-Fe-C). The significance of the variance with respect to the average per tap is shown in Figure 1 for Si which is one of the metallurgical important solutes (typical average values for silicon in a PAF is about 2%). The variation in the silicon assay was found to be very large (-90% to over 100% relative to the tap average). No clear pattern was visible as to the order in which positive and negative, large and small variations occurred. That is to say that large positive and negative variations may occur at the start of tapping, or at any time during tapping – sampling after half of the material has been tapped does not ensure a representative sample of the specific tap. Sampling based on one sample per tap can therefore not be representative. The Si assays shown in Figure 1 stem from taps from two sampling campaigns spaced 18 months from another. To establish the distribution of % relative variation for the different solution components, the relative variations per tap were combined for all taps, and a histogram was developed for each component.

The histogram of relative variation aids one to determine:

- If the distribution appears to be normal (Gaussian) and centred around a zero mean;
- The range of variation (maximum and minimum variation)
- The spread and the degree of central tendency

Moreover, it is revealing to compare the histograms for both the plasma arc furnace (PAF) and the submerged arc furnaces (SAF), as the mixing driving forces are different, even though similar alloys and slags are produced from chemically similar raw materials. Only the histograms of sulphur and silicon are shown in Figures 2-5 due to space constraints. The distributions tend to show Gaussian characteristics. The ranges of relative variation for the different components are, without exception, significantly larger for the PAF than for the SAF. As the frequent occurrence of larger relative variations in the melt constituents indicates poorer mixing, one may conclude that the HCFeCr alloy produced by the furnaces is poorer mixed in the PAF than in the SAF.

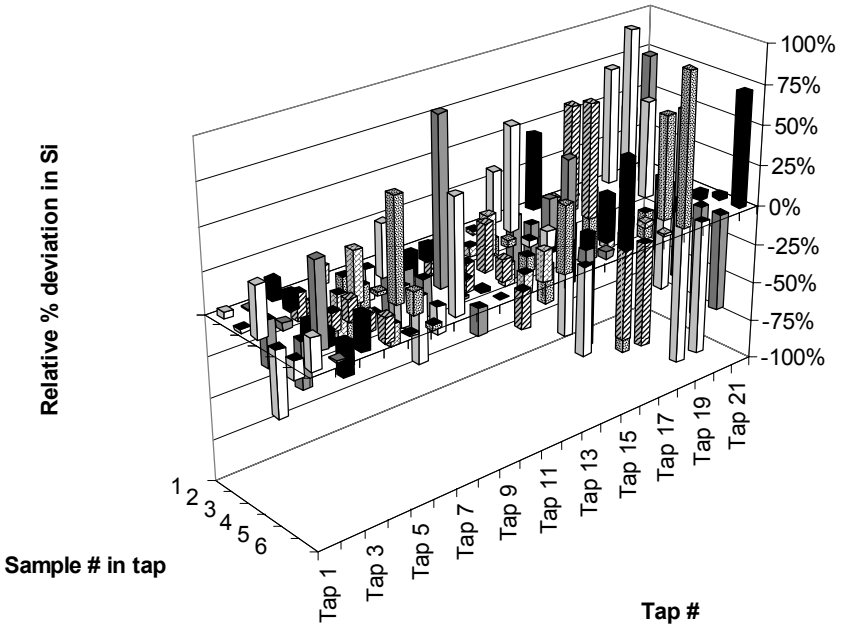

Figure 1. Sample by sample variation of silicon for a number of alloy taps (both campaigns for the PAF).

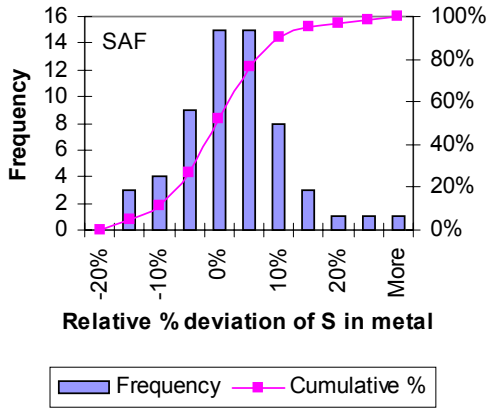

Figure 2. Distribution of sulphur in SAF-alloy.

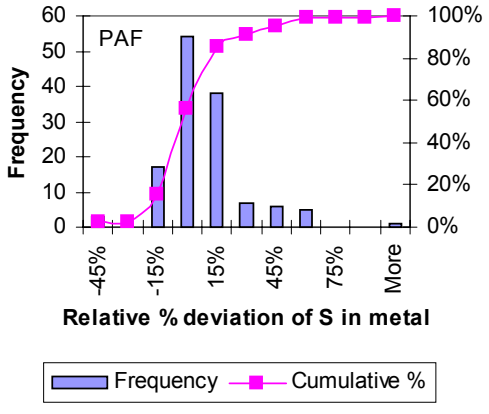

Figure 3. Distribution of sulphur in PAF-alloy.

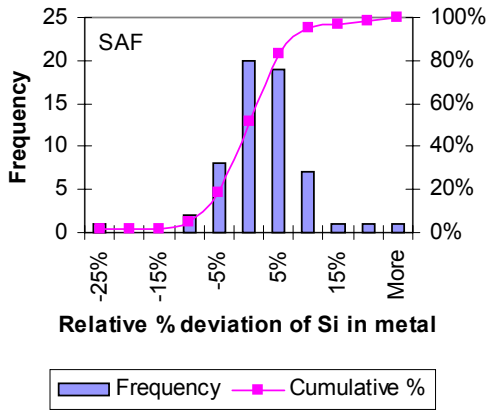

Figure 4. Distribution of silicon in SAF-alloy.

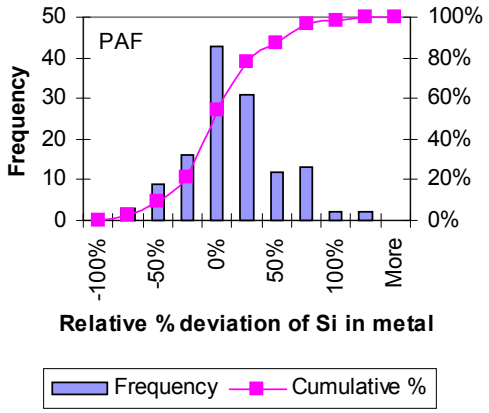

Figure 5. Distribution of silicon in PAF-alloy.

The poor alloy mixing in the PAF relative to the SAF is shown very clearly in Figure 6. Of all HCFeCr alloy elements Si and S are the least homogeneously distributed. As expected, the solvent components (Cr and C, Fe is not shown but is similar) are homogeneously distributed with associated low standard deviations. The standard deviations of all minor components are much larger than one can ascribe to analytical instrument error. Even though one might think that, due to the PAF being an open bath with in-bath reduction and gas generation, and plasma impingement on the bath, the PAF should be better stirred than the SAF, the measurements point towards the contrary. The relatively good alloy mixedness of the SAF system can be explained by the difference in electro-hydrodynamic forces acting between the two melt systems. In the case of the PAF, the single cathode electrical direct current flows in one direction only, with very little variation in the electrical and magnetic field strength. In the case of the alternating current 3 phase - 3 electrode SAF, an electrical star configuration (as opposed to the delta configuration) is formed. The dynamic resistance-inductance circuit (due to the dynamic nature of the AC circuit) has the anchor point of the star in the melt phase. This anchor point changes in position as the electrical phases change and the resistances vary. The creation of a variable and rotating induced magnetic field would therefore be able to serve as driving force to electro magnetically pump the conductive melt. It is not deemed within the scope of this paper to prove that this is the main mixing mechanism, but it is believed to be a plausible explanation.

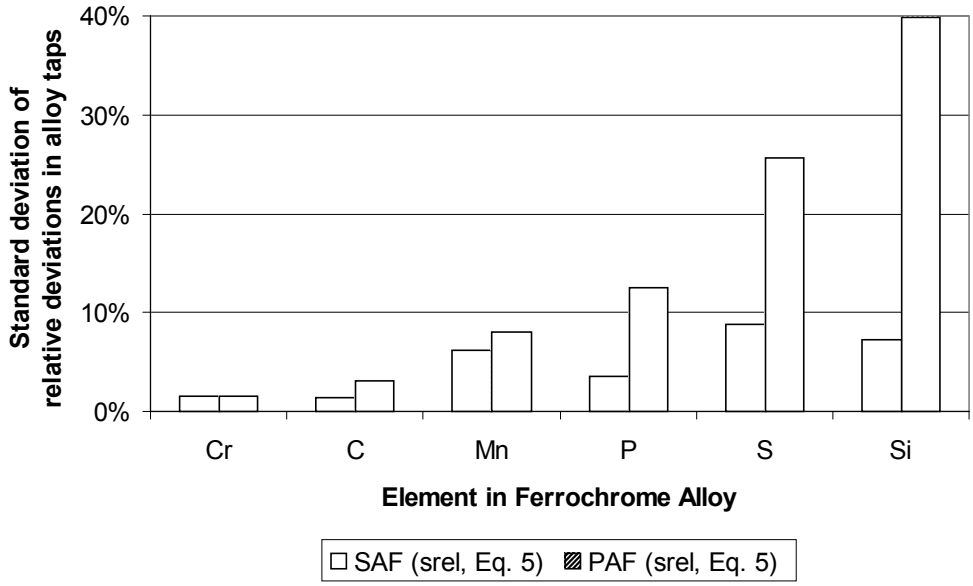

Figure 6. A comparison of the standard deviations of the relative deviations for alloy elements for submerged (SAF) and plasma (PAF) arc furnaces.

Even though silicon appears in appreciable quantities in HCFeCr melts (1-5%), it is the element that shows the largest degree of inhomogeneity. It was consequently decided to use silicon as identifier of mixedness. It was found that when the alloy melt was subcooled relative to the melt liquidus (as dictated by the average melt chemistry), the degree inhomogeneity increased (as measured by the standard deviation per tap in the relative Si deviation from the tap average). The phase equilibria and liquidus determination of the Fe-Cr-C-Si alloy melt system as investigated by Wethmar et al. [14], were used. For the PAF, there appears to be a decreasing linear relationship between the Si relative standard deviation per tap and increasing degrees of superheat associated with the tap, as clearly shown in Figure 7. A significant trend exists, which indicates that the inhomogeneity decreases with increasing superheat. However, other factors will also play a role (for example the electro-hydrodynamic effects). Figure 7 makes much sense when one considers that subcooling below the liquidus dramatically increases the viscosity due to partial melt crystallisation. As the alloy melt does not experience the effect of the plasma impingement on the melt surface, nor of gas bubbling due to oxide reduction reactions, as is the case for the slag, one would also expect that rheology becomes the overriding factor in determining melt homogeneity.

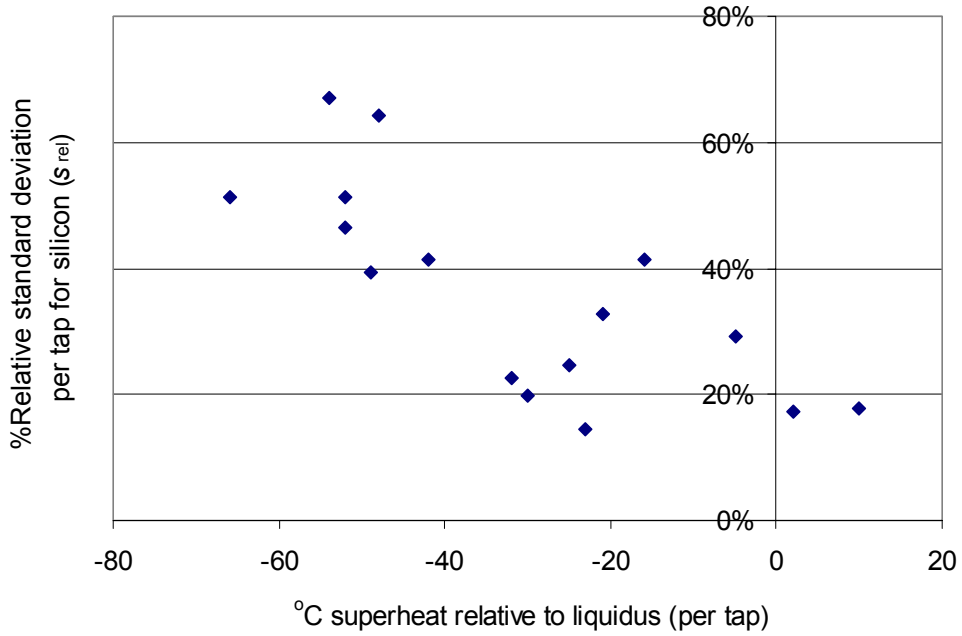

Figure 7. Relationship of unmixedness of the alloy, measured in terms of the relative standard deviation per tap in Si, to the degrees superheat of the alloy melt relative to the alloy liquidus.

4.2 Slag Homogeneity

The slag chemistry associated with ferrochrome production lies within the domain of the CaO-MgO-SiO_2-Al_2O_3 system, containing Fe and Cr in the M^0 (entrained), M^{+2} and M^{+3} (very little) oxidation states. Sulphur is normally dissolved as sulphide. None of the SEM-photos of slags investigated, show the presence of free carbon. In all cases it was associated with entrained alloy droplets.

Figure 8 shows how significant the Cr variation in the PAF-slag really is, relative to the average per tap. The samples from the first twelve tap numbers derive from the second campaign, while samples from tap numbers 13-21 derives from the first campaign, performed 18 months earlier, on the same furnace. Significant positive deviations (up to 80%) from the a specific tap-average occurred. The six samples per tap were ordered per tap according to their order of sampling, that is, the first sample per tap was taken the first moment fully developed flow through the launder was observed. The subsequent samples were then taken based on a equal time interval. The time intervals were determined based on the total durations of typical slag taps divided by 8 (6+2) to allow for the start and end periods during which no samples were taken. The sample position per tap where the maximum Cr-assay was observed varied from tap to tap. Neither did minimum deviations necessarily occur close to the middle of the tap. One can therefore not claim that sampling at any given time is more representative than at another instant. The assay-pattern is therefore truly stochastic. The histograms of the relative deviations for chromium in the SAF and PAF furnaces are shown in Figures 9 and 10, while the those for iron are shown in Figures 11 and 12.

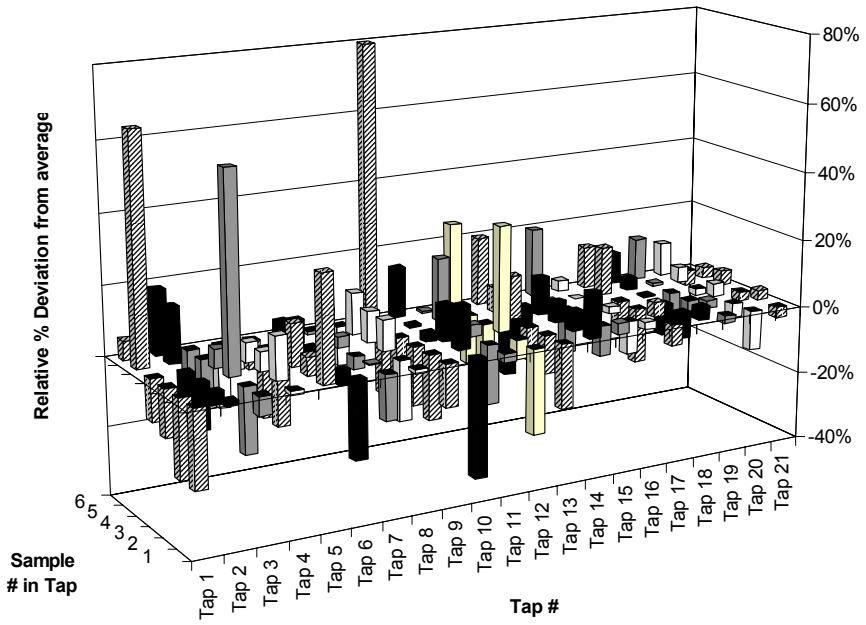

Figure 8. Sample by sample variation in Cr (as Cr_2O_3) within slags (both campaigns for the PAF).

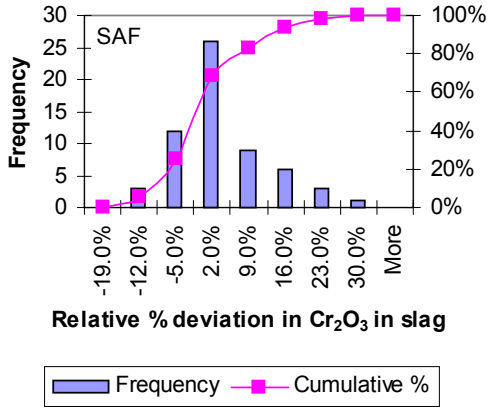

Figure 9. Distribution of Cr_2O_3 in SAF-slag.

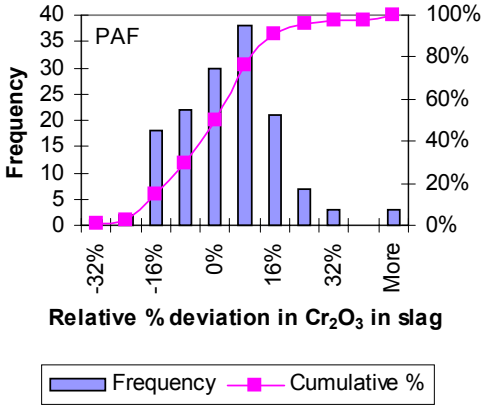

Figure 10. Distribution of Cr_2O_3 in PAF-slag.

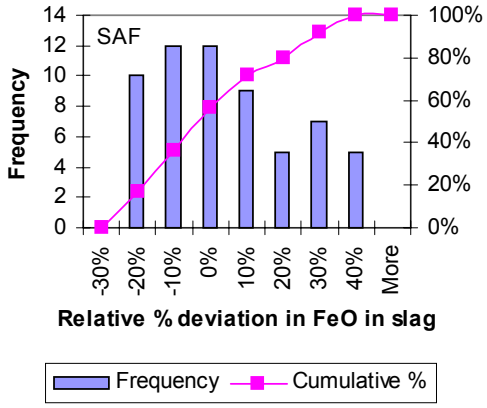

Figure 11. Distribution of FeO in SAF-slag.

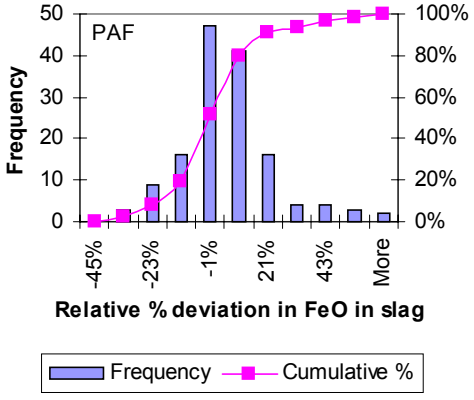

Figure 12. Distribution of FeO in PAF-slag.

Figures 9 tot 10 show that the distributions for PAF system in general tend to be close to normal, while the distributions of the SAF system are significantly skewed for FeO, (also CaO and SiO_2, although not showed). Most slag components show a comparative range and central tendency with the exception of CaO and Cr_2O_3, where large difference in composition deviation is apparent for the PAF and SAF and systems. The large variation in CaO could be ascribed to improper mixing in the burden of the SAF of the flux with the chromite and carbonaceous reductant, and the presence of undissolved limestone. Table 1 presents a summary of the standard deviations of the relative compositional variations of the different melts associated with HCFeCr production in SAF and PAF furnaces.

Table 1. A comparison of the standard deviation of the relative deviations of melt compositions for the submerged arc (SAF) and plasma arc (PAF) furnaces.

Slag	**Al_2O_3**	**CaO**	**Cr_2O_3**	**FeO**	**MgO**	**SiO_2**	**S**	**C**
SAF (s_{rel}, Eq. 5)	2.3%	13.8%	9.0%	19.3%	2.6%	4.4%	7.3%	52.7%
PAF (s_{rel}, Eq. 5)	2.8%	3.3%	15.7%	17.7%	2.4%	3.2%	5.3%	69.1%
Alloy	**Cr**	**C**	**Mn**	**P**	**S**	**Si**		
SAF (s_{rel}, Eq. 5)	1.5%	1.4%	6.1%	3.5%	8.8%	7.3%		
PAF (s_{rel}, Eq. 5)	1.6%	3.0%	8.0%	12.5%	25.6%	39.9%		

It is apparent that the slag from the PAF is well mixed with respect to the dissolved non-reduced oxides, but shows a very large degree of inhomogeneity with respect to components that are present (either totally or in part) as entrained phases.

5. MELT SPATIAL THERMAL DISTRIBUTIONS

Melt temperatures were logged based on continuous monitoring of the melt using the Mikron pyrometer. As expected, the temperature variation is much less than the composition variation of the solute components. In fact, the relative standard deviations of the melt temperatures are comparable in magnitude to the relative standard deviation of the solvent components, as is shown in Table 2. The low relative standard deviations supports the hypothesis that the thermal diffusivity is much larger than the mass diffusivity of the solute components in viscous melts. The larger thermal variation found in the PAF slag compared to the PAF alloy could be explained by the fact that the slag experiences extreme thermal gradients close to the arc attachment zone (AAZ), and close to the slag freeze line. The metal also conducts heat far better than the slag, and establishes thermal homogeneity much quicker.

Table 2. Maximum and average relative standard deviations in temperature for PAF and SAF melts.

Description	**Average**	**Maximum**
PAF, Alloy: Relative standard deviation (thermal)	1.6%	2.3%
PAF, Slag: Relative standard deviation (thermal)	1.8%	3.2%
SAF, Alloy: Relative standard deviation (thermal)	1.2%	2.8%
SAF, Slag: Relative standard deviation (thermal)	1.2%	2.8%

To compare the deviation patterns (from the tap averages) of silicon in the alloy and the associated temperatures, the average temperature associated with the time the sample was taken from the tap, was determined. These “sample average temperatures” were calculated based on the average temperature of the alloy between two alloy samples. This was done to have a similar number of temperature and composition measurements. The percentage deviations were then calculated relative to the tap average. The results for typical (not worst case) PAF and SAF taps are presented in Figures 13 and 14. In each case, the temperature deviation pattern is given to the right of the corresponding silicon deviation from the same tap.

From Figures 13 and 14, it should be noted that the scales of the axes differ by an order of magnitude. Moreover, there is no correlation between the chronology of the temperature deviation pattern and the silicon deviation pattern. For silicon in this particular case in the PAF, the major deviations occurred close to the middle of the tap, while the temperature deviated much more from the tap average initially and then again to

the end of the corresponding tap. For both alloy temperature and alloy composition the SAF showed lower variation in comparison to the PAF.

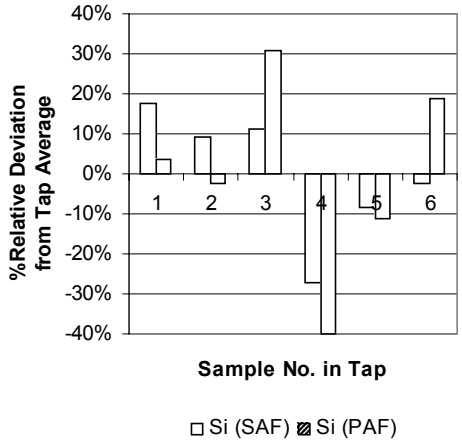

Figure 13. Deviation pattern of the silicon in the alloy for a selected PAF and a SAF tap.

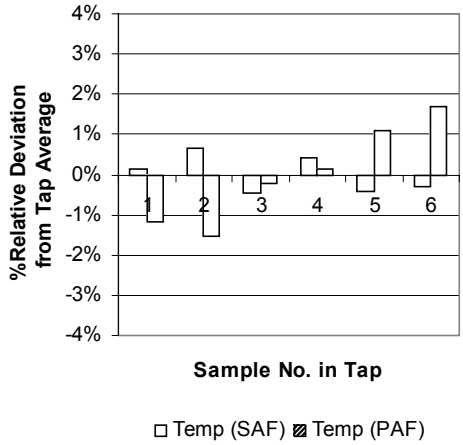

Figure 14. Deviation pattern of the alloy temperature for the same PAF and SAF taps shown in Figure 13.

As the metal and slag of the SAF are tapped simultaneously through the same tap hole (as opposed to the slag and alloy which are tapped consecutively through separate tap holes for the PAF) the metal and slag of the SAF shows the same thermal variance as well as overall temperatures. Based on the average standard deviation for all taps monitored (more than 10 taps in each case), one may conclude that, as was observed for composition, the SAF is also thermally better mixed than the PAF. It is interesting to note that the relative thermal deviation for the PAF is of similar magnitude to the relative thermal deviation predicted by Szekely *et al.* [6] for electric arc furnace steel making, based on CFD modelling techniques, if the thermal zones in the figure are graphically integrated according to their proportional contribution to the bulk temperature. It may therefore be concluded that, for HCFeCr production, both the PAF and SAF furnaces are, from a thermal perspective, well mixed.

6. CONCLUSIONS

Quantifying spatial heterogeneity, or mixedness, is required before on can commence with the development of process control models. If the distributed nature of melts is not taken into account it may result in gross errors when process data is used to develop semi-empirical models, or it may lead to rejecting fundamental models when they are validated against unrepresentative sample compositions. It was found that industrial open arc furnaces are not so well compositionally mixed as was predicted by CFD models. The main components showing significant variances in the alloys are the solute components, in particular silicon and sulphur. It was found that the degree of subcooling of the alloy melt relative to the liquidus had the largest identifiable impact on alloy mixedness. In general it was found that alloy mixedness in the submerged arc furnace was significantly better than for the alloy produced in an open arc furnace. In general the chromite smelting slags always had better mixedness than their corresponding alloys, for the solute species. On the other hand, precipitated or entrained compounds showed a very large variation throughout the volume of the furnace melt. It was found that the slag mixedness of the submerged and open arc furnaces are comparable. Despite the relatively poor mixing of the solute components, the melts were found to be thermally well mixed, which corresponds with CFD predictions. The discrepancy between thermal and compositional homogeneity was explained through the orders of magnitude difference between the thermal and mass diffusivity. Once the material variances for a pyrometallurgical reactor have been quantified, they can be used constructively in developing reconciled dynamic or steady state material balances which may be used in process control.

The authors have shown [1], [2], [3] that variance based material balance reconciliation, using the mixedness variances determined as presented in this paper, could be used to obtain material balance closure, while the reconciliation adjustments could also be estimated using dynamic process control models. Moreover, it was shown how the reconciled data could be used, together with fundamental thermodynamic models, inventory models and a final systems model, to predict the actual melt chemistry of the subsequent tap within the inherent variance associated with the variable.

7. REFERENCES

[1] Eksteen, J.J., Frank, S.J., Reuter, M.A., "Dynamic structures in variance based data reconciliation adjustments for a chromite smelting furnace", Minerals Engineering, Vol. 15, No. 11, pp. 931-943, 2002.

[2] Reuter, M.A., Eksteen, J.J., Van Schaik, A., "Pyrometallurgical Reactors – Closers of the recycling materials cycle", Proceedings of the Yazawa International Symposium on Metallurgical Materials Processing: Principles and Technologies, Ed. F. Kongoli, K. Itagaki, and H.Y.Sohn, TMS, March 3-7, San Diego, California, USA, pp. 1005-1017, 2003.

[3] Eksteen, J.J. and Reuter, M.A., "A generic approach to the development of semi-empirical predictive models for bath type furnaces", Proceedings of the XXII International Mineral Processing Congress, 28 Sep. - 3 Oct. 2003, Cape Town, South Africa, Accepted for publication.

[4] Georgalli, G.A. Eksteen, J.J. and Reuter, M.A., "An Integrated Thermochemical-Systems Approach to the Prediction of Matte Composition Dynamics in an Ausmelt Nickel-Copper Matte Converter", Minerals Engineering, 15(11), pp. 909-917, 2002.

[5] Gunnewick, L.H. and Tullis, S., "Prediction of heat and fluid flow in the slag phase of an electric arc furnace", Proceedings of the International Symposium on Computational Fluid Mechanics and Heat/Mass Transfer Modelling in the Metallurgical Industry, Eds. S.A. Argyropoulos and F. Mucciardi, August 24-29, Montreal, Quebec, CIM, pp., 250-264, 1996.

[6] Szekely, J., McKelliget, J., and Choudhary, M., "Heat transfer, fluid flow, and bath circulation in electric arc furnaces and DC plasma furnaces", Iron and Steelmaking, Vol. 10, No. 4, pp. 169-179, 1983.

[7] Qian, F., Farouk, B., and Mutharasan, R., "Modelling of fluid flow and heat transfer in the plasma region of the DC electric arc furnace", Metallurgical and Material Transactions B, 26B, pp. 1057-1067, 1995.

[8] Cafferey G., Warnica, D., Molloy, N., and Lee, M., "Temperature homogenisation in an electric arc furnace steel bath", International Conference on CFD in Mineral and Metal Processing and Power Generation, CSIRO, pp. 87-99, 1997.

[9] Larsen, H.L., Gu, L., and Bakken, J.A., "A numerical model for the AC arc in the silicon melting furnace", INFACON VII, Ed., Tuset, Tveit, and Page, Trondheim, Norway, pp. 517-527, 1995.

[10] Harnby, N., Edwards, M.F., Nienow, A.W., "Mixing in the process industries", Butterworths, London, 1985.

[11] Levenspiel, O., "Chemical Reaction Engineering", 2nd Edition, Wiley, 1972

[12] Beyer, W.H., "Handbook of tables for probability and statistics", 2nd Ed., CRC Press, 1968

[13] Turkdogan, E.T., "Physicochemical properties of slags and glasses", The Metals Society, London, 1983

[14] Wethmar, J.C.M., Howat, D.D., Jochens, P.R., "Phase equilibria in the Cr-Fe-Si-C system in the composition range representative of high carbon ferrochromium alloys produced in South Africa", Metal Science, Vol. 9, pp. 291-296, 1975.